# Effect of Morphology on Electron Transport in Dye-Sensitized Nanostructured TiO₂ Films

Nam-Gyu Park[a]*, Jao van de Lagemaat[b], and Arthur J. Frank[b]

[a]Basic Research Lab., Electronics and Telecommunications Research Institute (ETRI), Daejeon 305-350, South Korea
[b]National Renewable Energy Laboratory (NREL), Golden, CO 80401, USA

The relationship between the morphology of nanostructured TiO₂ films and the photo-injected electron transport has been investigated using intensity-modulated photocurrent spectroscopy (IMPS). For this purpose, three different TiO₂ films with 5 μm thickness are prepared: The rutile TiO₂ film with 500 nm-sized cluster-like spherical bundles composed of the individual needles (T1), the rutile TiO₂ film made up of non-oriented, homogeneously distributed rod-shaped particles having a dimension of approximately 20×80 nm (T2), and the anatase TiO₂ film with 20 nm-sized spherically shaped particles (T3). Cross sectional scanning electron micrographs show that all of the TiO₂ films have a quite different particle packing density: poorly packed T1 film, loosely packed T2 film and densely packed T3 film. The electron transport is found to be significantly influenced by film morphology. The effective electron diffusion coefficient $D_{eff}$ derived from the IMPS time constant is an order of magnitude lower for T2 than for T3, but the $D_{eff}$ for the T1 sample is much lower than T2. These differences in the rate of electron transport are ascribed to differences in the extent of interparticle connectivity associated with the particle packing density.

**key words:** dye-sensitized, nanocrystalline, TiO₂, IMPS (Intensity Modulated Photocurrent Spectroscopy), electron transport

## INTRODUCTION

Interest in the study of dye-sensitized nanocrystalline metal oxide solar cells has grown notably in recent years from both a fundamental and an applied perspective. The nanometer-sized crystallites, which are interconnected, are the recipient of injected electrons from optically excited dye molecules and provides the conductive pathway from the site of electron injection to the transparent back contact [1]. Regeneration of the dye takes place with a redox electrolyte. During photo-injected electrons traverse the nanoparticle network, not all of the injected electrons are collected at the back contact; some may react (recombine) with redox species (e.g., I₃⁻) or dye molecules at the particle/electrolyte interface. Since the collection of electrons competes with recombination, slow electron transport can lead to a low charge-collection efficiency and hence a low solar-to-electrical conversion efficiency [2,3]. In this context, the rate of electron transport is a major determinant of the overall efficiency of dye-sensitized nanocrystalline TiO₂ solar cells. The investigation of factors affecting electron-transport kinetics is thus important for improving cell performance. For instance, the chemical bonding nature between dye molecules and TiO₂,

the morphology of the nanostructured TiO₂ films, and the redox electrolyte can be all indispensable to influencing the electron transport.

Intensity-modulated photocurrent spectroscopy (IMPS) provides the information on the kinetics of the electron transport and has been studied in nanocrystalline TiO₂ films [2, 4-7]. Electron transport has been modeled in terms of an effective electron diffusion coefficient ($D_{eff}$) [7,8] because of the absence of a significant electrical potential gradient in the film [2, 4-11], and the time constants for IMPS ($\tau_{IMPS}$) have been correlated with $D_{eff}$ [2,4,7,12].

In this paper, we report on an effect of the TiO₂ film morphology on the electron transport in terms of an effective electron diffusion coefficient, based on our previous results on the dye-sensitized anatase and rutile TiO₂ solar cells [13,14]. Electron diffusion coefficients, obtained from the data measured by IMPS, of three different TiO₂ films sensitized with Ru-based dye molecules are compared.

## MATERIALS AND METHODS

The TiO₂ films with different morphology were prepared as follows: 1) Rutile TiO₂ particles formed from the hydrolysis of TiCl₄ were directly deposited on the surface of transparent SnO₂ conducting glass (Libbey-Owens-Ford Co., TEC-8 (8 ohm/sq), 75% transmittance in the visible) and then heated in air for 1 h at 500°C [13]. 2) Rutile TiO₂ particles were prepared as a slurry and

then deposited onto the glass substrate with a doctor blade and then heated in air for 1 h at 500°C. The method for making a slurry was reported elsewhere [14]. 3) Nanocrystalline anatase $TiO_2$ films were prepared by depositing a colloidal anatase $TiO_2$, prepared by the hydrolysis of titanium tetraisopropoxide in the presence of acetic acid [15], onto the conducting glass substrate as detailed elsewhere [16]. The measured film thicknesses with a Tencor Alpha-step profiler were ca. 5 μm.

The morphology of $TiO_2$ films was investigated by field emission scanning electron microscopy (SEM; JEOL Model 6320F)

For photosensitization, the $TiO_2$ electrodes were immersed in acetonitrile/t-butanol (50:50 v/v%) containing $3\times10^{-4}$ M $Ru(LL')(NCS)_2$ (where L=2,2'-bypyridyl-4,4'-dicarboxylic acid, and L'=2,2'-bipyridyl-4,4'-ditetrabutylammoniumcarboxylate) for 24 h at room temperature. The dye-covered electrodes were then rinsed with the acetonitrile/t-butanol mixture and dried under a $N_2$ stream. A 60-nm thick Pt film on top of a 40 nm layer of Ti on a glass plate was used as a counter electrode. The redox electrolyte, consisting of 0.6 M 1,2-dimethyl-3-hexyl imidazolium iodide, 0.2 M LiI, 40 mM $I_2$, and 0.2 M tert-butyl pyridine in acetonitrile, was introduced into the assembled cell.

The setup for the intensity-modulated photocurrent spectroscopy (IMPS) measurements is described elsewhere [2]. In the IMPS studies, the samples were illuminated with 680-nm wavelength light, which is only weakly absorbed by the dye.

## RESULTS AND DISCUSSION

In Figure 1, top and cross sectional SEM micrographs show the morphology of the three different type of the $TiO_2$ films. Each film has a unique morphology. The directly deposited rutile $TiO_2$ film (T1) consists of cluster-like spherical bundles with an average dimension of about 500 nm (Fig. 1(a)). The individual needles with a dimension of approximately 20×80 nm appear to radiate out from the bundles. The slurry-based rutile $TiO_2$ film (T2) in Figure 1(c) is made up of non-oriented, homogeneously distributed rod-shaped particles having an average dimension of 20×80 nm. Figure 1(e) shows the anatase $TiO_2$ film (T3) with the spherically shaped anatase particles (20-nm diameter). The cross sectional SEM micrographs in Figure 1(b,d and f) reveal that the direct deposit of rutile $TiO_2$ particles leads to poor packing across the film layer (see Fig. 1 (b)), on the other hand, the slurry-based rutile and anatse $TiO_2$ films exhibit a close-packing of individual particle. The anatase $TiO_2$ particles (Fig. 1(f)) are packed more densely than the rutile particles in the slurry-based rutile $TiO_2$ film (Fig. 1(d)).

Figure 2 shows the effective electron diffusion coefficient ($D_{eff}$) as a function of light intensity at 680-nm illumination represented by photocurrent density ($J_{sc}$) for dye-sensitized 5 (m-thick $TiO_2$ films with different morphology. $D_{eff}$ is calculated from the relation $D_{eff}=d^2/4\tau_{IMPS}$. This equation is valid only in the absence of recombination and for

homogeneously absorbed light. Recombination is not important at short circuit for dye-sensitized solar cells for film thicknesses used in this study [2,3,14]. In Figure 2, it can be seen that at the same $J_{sc}$ the effective electron diffusion coefficient $D_{eff}$ for T1 is about $10^{1.5}$ times lower than that for T2, and $D_{eff}$ for T2 is about an order of magnitude lower than that for T3, implying that electron transport becomes faster on going from T1 to T2 and T3 electrode. When comparing the densely packed 20-nm anatase particle film (T3) and the relatively loosely packed 20×80 nm rutile film (T2), the difference in the rate of electron transport in these materials could be due to different densities of surface states or the extent of interparticle connectivity. We first ponder the possible role of surface states. It is generally accepted that the transport of electrons through the nanostructured film is slowed down by multiple trapping events, involving principally surface states [5,6,11,12]. The number of surface states is generally proportional to the surface area of a film. If the number of surface states were the primary basis of the difference in the rate of electron transport in these materials, then one would expect that the surface area of the rutile film would be substantially larger than that of anatase. However, a comparison of the cross sectional SEM micrographs in Figure 1(d and f) shows just the opposite, as discussed above. The surface area of the rutile film is smaller than that of the anatase film. On this basis, one would predict that electron
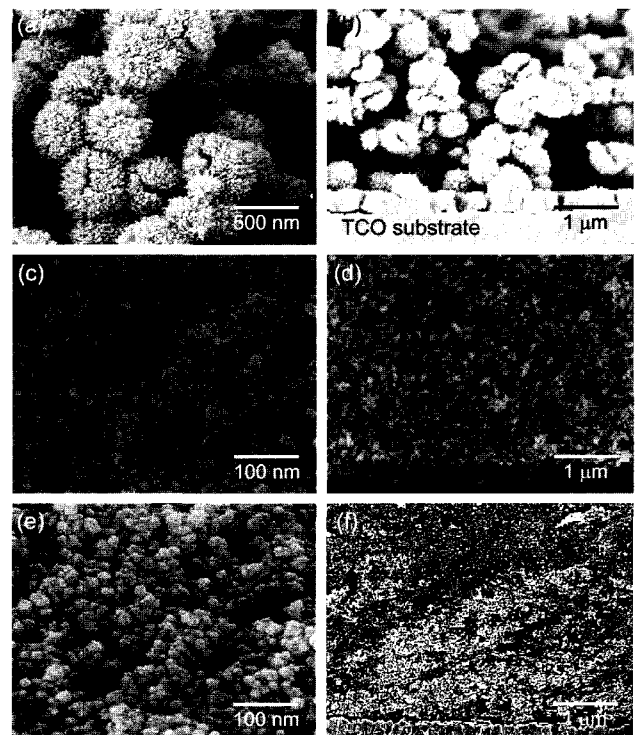


Figure 1. Surface and cross sectional SEM micrographs of (a and b) the directly deposited rutile $TiO_2$ film T1, (c and d) the slurry-based rutile $TiO_2$ films T2, and (e and f) the slurry-based anatase $TiO_2$ film T3 coated on conducting glass and annealed at 500°C for 1 h
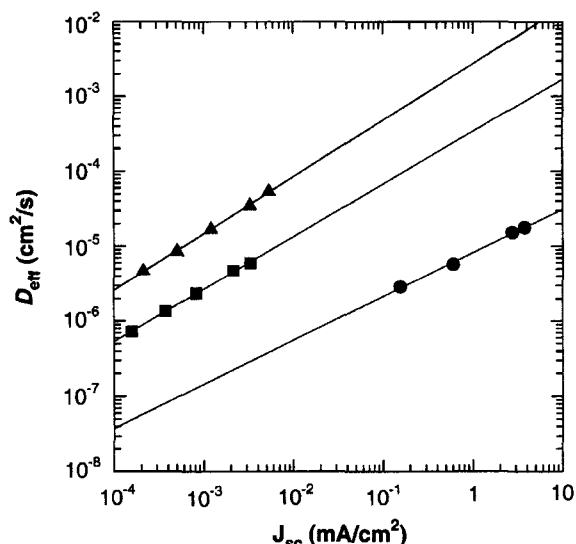
Figure 2. Comparison of the electron diffusion coefficient $D_{eff}$ of dye-sensitized $TiO_2$ films of the same thickness (5 μm) as a function of the short-circuit current density $J_{sc}$ at 680-nm illumination: symbols (●), (■) and (▲) represent $D_{eff}$'s of T1, T2, and T3, respectively, and solid lines are linear regression result.

transport would be faster in rutile than in anatase, which is contrary to the data in Figure 2. This suggests that the difference in the rate of electron transport in these materials may be due to the extent of interparticle connectivity. In support of this possibility, a comparison of the morphology for the slurry-based rutile (T2) and anatase (T3) films implies that within a given area or volume element, the number of non-spherically shaped, large sized (20×80 nm) rutile particles is less than that of the spherically shaped, small sized (20-nm diameter) anatase particles. These considerations lead to the conclusion that the rutile particles stack less efficiently than the anatase particles and that the rutile films have a lower density of interparticle connections per cell volume than that of the anatase film. Thus the number of pathways encountered by an individual electron en route to the collecting electrode is effectively smaller for a rutile film than for an anatase film. Restricting the number of conductive pathways through the particle network is expected to slow electron transport through the rutile film and lower the electron diffusion coefficient. Based on the above interpretation, the much slower electron transport in the directly deposited rutile $TiO_2$ film (T1) is as a consequence of the poor interparticle connectivity through the film distance.

## CONCLUSION

The electron transport of the dye-sensitized $TiO_2$ solar cells are strongly influenced by the film morphology. Analyses of intensity-modulated photocurrent spectroscopy and scanning electron microscopy data suggest that electron transport is

significantly dependent on the extent of interparticle connectivity associated with the particle packing density. Increasing the particle packing density as well as increasing the surface area by producing a densely packed film of nanosized particles is therefore expected to improve the photoconversion efficiency in dye-sensitized nanocrystalline semiconductor solar cells.

## REFERENCES

1. Hagfeldt, A. and Gratzel, M. (1995) Light-Induced Redox Reactions in Nanocrystalline Systems. *Chem. Rev.*, 49-68
2. Schlichthorl, G., Park, N.-G. and Frank, A. J. (1999) Evaluation of the Charge-Collection Efficiency of Dye-Sensitized Nanocrystalline $TiO_2$ Solar Cells. *J. Phys. Chem. B*, **103**, 782-791
3. van de Lagemaat, J., Park, N.-G. and Frank, A.J. (2000) Influence of Electrical Potential Distribution, Charge Transport, and Recombination on the Photopotential and Photocurrent Conversion Efficiency of Dye-Sensitized Nanocrystalline $TiO_2$ Solar Cells: A Study by Electrical Impedance and Optical Modulation Techniques. *J. Phys. Chem. B*, **104**, 2044-2052
4. Cao, F., Oscam, G., Meyer, G. J. and Searson, P. C. (1996) Electron Transport in Porous Nanocrystalline $TiO_2$ Photoelectrochemical Cells. *J. Phys. Chem.*, **100**, 17021-17027
5. de Jongh, P.E. and Vanmaekelbergh, D. (1996) Trap-Limited Electronic Transport in Assemblies of Nanometer-Size $TiO_2$ Particles. Phys. Rev. Lett., **77**, 3427-3430
6. de Jongh, P. E., Vanmaekelbergh, D. (1997) Investigation of the Electronic Transport Properties of Nanocrystalline Particulate $TiO_2$ Electrodes by Intensity-Modulated Photocurrent Spectroscopy. *J. Phys. Chem. B*, **101**, 2716-2722
7. Dloczik, L., Ileperuma, O., Lauermann, I., Perer, L. M., Ponomarev, E. A., Redmond, G., Shaw, N. J. and Uhlendorf, I. (1997) Dynamic Response of Dye-Sensitized Nanocrystalline Solar Cells: Characterization by Intensity-Modulated Photocurrent Spectroscopy. *J. Phys. Chem. B*, **101**, 10281-10289
8. Solbrand, A., Lindstrom, H., Rensmo, H., Hagfeldt, A., Lindquist, S.-E. and Sodergren, S. (1997) Electron Transport in the Nanostructured $TiO_2$-Electrolyte System Studied with Time-Resolved Photocurrents. *J. Phys. Chem. B*, **101**, 2514-2518
9. Schwarzburg, K. and Willig, F. (1999) Origin of Photovoltage and Photocurrent in the Nanoporous Dye-Sensitized Electrochemical Solar Cell. *J. Phys. Chem. B*, **103**, 5743-5746
10. Bisquert, J., Garcia-Belmonte, G. and Fabregat-Santiago, F. (1999) Modelling the Electric Potential Distribution in the Dark in Nanoporous Semiconductor Electrodes. *J. Solid State Electrochem.*, **3**, 337-347

11. Nelson, J. (1999) Continuous-time Random-walk Model of Electron Transport in Nanocrystalline TiO₂ Electrodes. *Phys. Rev. B*, **59**, 15374-15380

12. Kopidakis, N., Schiff, E. A., Park, N.-G., van de Lagemaat, J. and Frank, A. J. (2000) Ambipolar Diffusion of Photocarriers in Electrolyte-Filled, Nanoporous TiO₂. *J. Phys. Chem. B*, **104**, 3930-3936

13. Park, N.-G., Schlichthörl, G., van de Lagemaat, J., Cheong, H.M., Mascarenhas, A. and Frank, A. J. (1999) Dye-Sensitized TiO₂ Solar Cells: Structural and Photoelectrochemical Characterization of Nanocrystalline Electrodes Formed from the Hydrolysis of TiCl4. *J. Phys. Chem. B*, **103**, 3308-3314

14. Park, N.-G., van de Lagemaat, J. and Frank, A. J. (2000) Comparison of Dye-Sensitized Rutile- and Anatase-Based TiO₂ Solar Cells. *J. Phys. Chem. B*, **104**, 8989-8994

15. Zaban, A., Ferrere, S., Sprague, J. and Gregg, B. A. (1997) pH-Dependent Redox Potential Induced in a Sensitizing Dye by Adsorption onto TiO₂. *J. Phys. Chem. B*, **101**, 55-57

16. Huang, S. Y., Schlichthörl, G., Nozik, A. J., Gratzel, M. and Frank, A. J. (1997) Charge Recombination in Dye-Sensitized Nanocrystalline TiO₂ Solar Cells. *J. Phys. Chem. B*, **101**, 2576-2582